

Substrate nitridation induced modulations in transport properties of wurtzite GaN/p-Si (100) heterojunctions grown by molecular beam epitaxy

Thirumaleshwara N. Bhat, Mohana K. Rajpalke, Basanta Roul, Mahesh Kumar, and S. B. Krupanidhi

Citation: *J. Appl. Phys.* **110**, 093718 (2011); doi: 10.1063/1.3658867

View online: <http://dx.doi.org/10.1063/1.3658867>

View Table of Contents: <http://jap.aip.org/resource/1/JAPIAU/v110/i9>

Published by the [American Institute of Physics](http://www.aip.org).

Related Articles

Rapid hot-electron energy relaxation in lattice-matched InAlN/AlN/GaN heterostructures

Appl. Phys. Lett. **102**, 062104 (2013)

Electrical and interfacial properties of GaAs/GaSb metal-organic vapour phase epitaxy heterostructures

J. Appl. Phys. **113**, 043719 (2013)

Band offset determination of mixed As/Sb type-II staggered gap heterostructure for n-channel tunnel field effect transistor application

J. Appl. Phys. **113**, 024319 (2013)

Split-gate quantum point contacts with tunable channel length

J. Appl. Phys. **113**, 024507 (2013)

Tunnel conductance in GaN:Mn/AlN/GaN:Mn (0001) junction from first-principles calculations

J. Appl. Phys. **112**, 123711 (2012)

Additional information on J. Appl. Phys.

Journal Homepage: <http://jap.aip.org/>

Journal Information: http://jap.aip.org/about/about_the_journal

Top downloads: http://jap.aip.org/features/most_downloaded

Information for Authors: <http://jap.aip.org/authors>

ADVERTISEMENT



AIP Advances

Now Indexed in
Thomson Reuters
Databases

Explore AIP's open access journal:

- Rapid publication
- Article-level metrics
- Post-publication rating and commenting

Substrate nitridation induced modulations in transport properties of wurtzite GaN/p-Si (100) heterojunctions grown by molecular beam epitaxy

Thirumaleshwara N. Bhat,¹ Mohana K. Rajpalke,¹ Basanta Roul,^{1,2} Mahesh Kumar,^{1,2} and S. B. Krupanidhi^{1,a)}

¹Materials Research Centre, Indian Institute of Science, Bangalore- 560012, India

²Central Research Laboratory, Bharat Electronics, Bangalore-560013, India

(Received 12 August 2011; accepted 6 October 2011; published online 9 November 2011)

Phase pure wurtzite GaN films were grown on Si (100) substrates by introducing a silicon nitride layer followed by low temperature GaN growth as buffer layers. GaN films grown directly on Si (100) were found to be phase mixtured, containing both cubic (β) and hexagonal (α) modifications. The x-ray diffraction (XRD), scanning electron microscopy (SEM), photoluminescence (PL) spectroscopy studies reveal that the significant enhancement in the structural as well as in the optical properties of GaN films grown with silicon nitride buffer layer grown at 800 °C when compared to the samples grown in the absence of silicon nitride buffer layer and with silicon nitride buffer layer grown at 600 °C. Core-level photoelectron spectroscopy of Si_xN_y layers reveals the sources for superior qualities of GaN epilayers grown with the high temperature substrate nitridation process. The discussion has been carried out on the typical inverted rectification behavior exhibited by n-GaN/p-Si heterojunctions. Considerable modulation in the transport mechanism was observed with the nitridation conditions. The heterojunction fabricated with the sample of substrate nitridation at high temperature exhibited superior rectifying nature with reduced trap concentrations. Lowest ideality factors (~ 1.5) were observed in the heterojunctions grown with high temperature substrate nitridation which is attributed to the recombination tunneling at the space charge region transport mechanism at lower voltages and at higher voltages space charge limited current conduction is the dominating transport mechanism. Whereas, thermally generated carrier tunneling and recombination tunneling are the dominating transport mechanisms in the heterojunctions grown without substrate nitridation and low temperature substrate nitridation, respectively. © 2011 American Institute of Physics. [doi:10.1063/1.3658867]

INTRODUCTION

The growth of device quality GaN based heterostructures on Si substrates is of huge interest in terms of cost, availability, processing, and integration.¹⁻³ Hexagonal GaN has been already successfully deposited on Si (111) substrates either by metalorganic chemical vapor deposition⁴ (MOCVD) or by molecular beam epitaxy^{2,3} (MBE) methods, in spite of the difficulties related to the very high reactivity of the silicon surface with nitrogen, the large lattice mismatch (-16.2%), and the large difference in thermal expansion coefficient (113%). However, from the point of view of integrating GaN devices with silicon technology, the Si (100) substrate is preferred as it is the most widely used in silicon mainstream technology.

Contrary to the (111) plane, the (100) plane of silicon does not possess a sixfold symmetry but a fourfold symmetry, which is more suitable for the epitaxial growth of a cubic phase. Nevertheless, the (β -GaN) cubic phase is metastable, and the thermodynamically stable hexagonal GaN phase could be grown on the (100) plane. A few attempts to grow compact epilayers of GaN on Si (100) aimed either to obtain pure cubic phase GaN (Ref. 1) or wurtzite GaN avoiding cubic inclusions by means of complex buffer structures.² Wurtzite GaN films

were grown on silicon nitride buffer layers formed on Si (111) substrates by radio frequency - MBE (RF-MBE) (Ref. 3) and concluded that the single crystalline wurtzite GaN was grown on the buffer layers of stoichiometric silicon nitride buffer layers.

Recently we reported the negative differential capacitance behavior in n-GaN/p-Si heterojunctions.⁵ However, to our knowledge no previous report is evident on the transport characteristic studies of the GaN/p-Si heterojunction and the effect of substrate nitridation on it. This report focuses on the effect of substrate nitridation and substrate nitridation temperature on structural and optical properties of wurtzite GaN films grown on Si (100) substrates followed by detailed transport properties of the GaN/p-Si heterojunction.

EXPERIMENTAL

The MBE system employed in this series of growth is equipped with the radio-frequency nitrogen plasma source. The GaN films were grown under a base vacuum better than 1×10^{-10} mbar on ultrasonically cleaned p-Si (100) wafers etched with 10% hydrofluoric acid followed by thermal cleaning at 900 °C under UHV for 1 h. Three samples were grown in the present series at different nitridation conditions, viz., in the absence of substrate nitridation, grown with substrate nitridation at 600 °C and substrate nitridation at 800 °C. The duration of substrate nitridation was 30 min and

^{a)}Author to whom correspondence should be addressed. Electronic mail: sbk@mrc.iisc.ernet.in.

was carried out by employing the nitrogen plasma. The nitrogen flow rate, RF-plasma powers were kept at 0.5 sccm, 350 W for substrate nitridation and for all the growths. Other than these parameters, the Gallium beam equivalent pressure (BEP) was maintained at 5.6×10^{-7} mbar for the whole series. The growth of the GaN buffer layer was carried out at the temperature of 500 °C for 15 min followed by the high temperature epilayer growth. The high temperature growth was carried out at 650 °C for 3 h. The structural characterizations of the as grown samples were carried out by x-ray diffraction (XRD) and scanning electron microscopy (SEM). Core-level photoelectron spectroscopy was carried out to analyze the nature of the Si_xN_y layer. Besides, the emission properties of the GaN films were investigated by room temperature photoluminescence (RT PL) spectroscopy using the 325 nm line of a He-Cd laser as an excitation source. The aluminum contact metallization on Si and GaN was done by thermal evaporation technique for transport studies. The contacts were annealed at 200 °C for 15 min for better adhesion to the film. The device transport characteristics were studied at room temperature using the probe station attached with the KIETHLY 236 source measure unit.

RESULTS AND DISCUSSION

Figure 1 shows the XRD pattern obtained for all the three samples. Samples grown without substrate nitridation depict the phase mixed nature (Fig. 1(a)), i.e., zinc blende (002) and wurtzite (0002) at 40° and 34.5°,⁶ respectively. Figures 1(b) and 1(c) show the XRD pattern of the samples grown with low and high temperature substrate nitridation, respectively, phase pure wurtzite (0002) reflection without any inclusions of cubic phase was obtained. The full width at half maximum (FWHM) of the (0002) peak of samples grown in the absence of substrate nitridation, low temperature nitridation, and high temperature nitridation are given by 0.148°, 0.131°, 0.106°, respectively. The peak intensity corresponding to the GaN (0002) increased with the substrate nitridation temperature.

The nitridation of the Si surface at high temperature causes the formation of the Si_xN_y buffer layer³ which breaks off the perfect registry between Si (100) (which exhibits fourfold symmetry) and GaN, and avoids⁶ the nucleation of β -GaN (cubic). On the other hand, the direct growth of GaN on Si also causes the amorphous Si_xN_y patches (regions) at

the interface due to the high reactivity of Si and N.⁶ The nucleation and initial growth of α -GaN occurs on top of these regions. In addition to this, the interfacial regions where GaN and Si are not in perfect registry with each other, misoriented GaN grains together with a high density of stacking faults can also induce the nucleation of α -GaN. Other than these two regions, the nucleation of cubic (β)-GaN occurs,⁶ causing a phase mixture. Hence the nitridation of the Si surface favors the growth of wurtzite GaN. The morphological SEM images are shown in Fig. 2 for all the three samples. The images reveal nano sized grain distribution of the GaN thin films grown at different nitridation conditions. While the films grown at high temperature nitridation were densely packed, the films grown at low temperature nitridation and absence of nitridation tended to be slightly porous. This could be explained as follows: The crystalline quality of the stoichiometric Si_3N_4 layer increases as the temperature of nitridation increases which provides better under layer for the growth of GaN epitaxy.

Core-level photoelectron spectroscopy was carried out to determine the sources for the superior quality of GaN epilayers. The chemical bonding states of the Si_xN_y surface was determined using Al K α ($h\nu=1486.6$ eV) radiation. Figure 3 shows the Si 2p core-level spectra for Si_xN_y layers formed at the nitridation temperature of 600 °C and 800 °C, respectively. The core-level spectra have been numerically fitted using Lorentzian convoluted with a Gaussian function. A Si atom is bonded to 4 N atoms (Si^{4+}) and a N atom is bonded to 3 Si atoms in the stoichiometric silicon nitride.⁷ Hence only the component with Si^{4+} is expected. But at the interface, two more coordinations are required, namely, Si^{3+} and Si^{1+} , for an ideal matching between the silicon nitride and Si lattices.⁸ The decomposition is shown in the figure, with one bulk along with three other components. The binding energies with respect to bulk position are at +0.61, +2.23, +3.09 eV for Si^{1+} , Si^{3+} , and Si^{4+} , respectively. Similar work has been reported by Lee *et al.*⁹ recently. The approximate ratios between the Si^{1+} , Si^{3+} , and Si^{4+} components are 0.3:0.3:0.4 and 0.2:0.1:0.7 for the Si_xN_y layers of the samples of low and high temperature substrate nitridations, respectively. Hence the intensity of the stoichiometric component has drastically been increased in the sample of high temperature nitridation. Collectively one can conclude that the quality of the silicon nitride layer notably affects the properties of GaN epilayers.

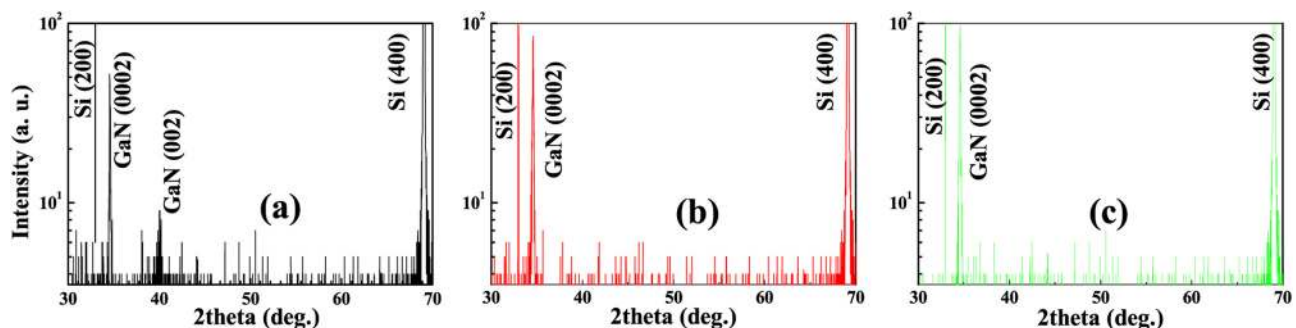


FIG. 1. (Color online) The HRXRD pattern of the GaN films grown with (a) absence of nitridation, (b) nitridation at 600 °C, and (c) nitridation at 800 °C.

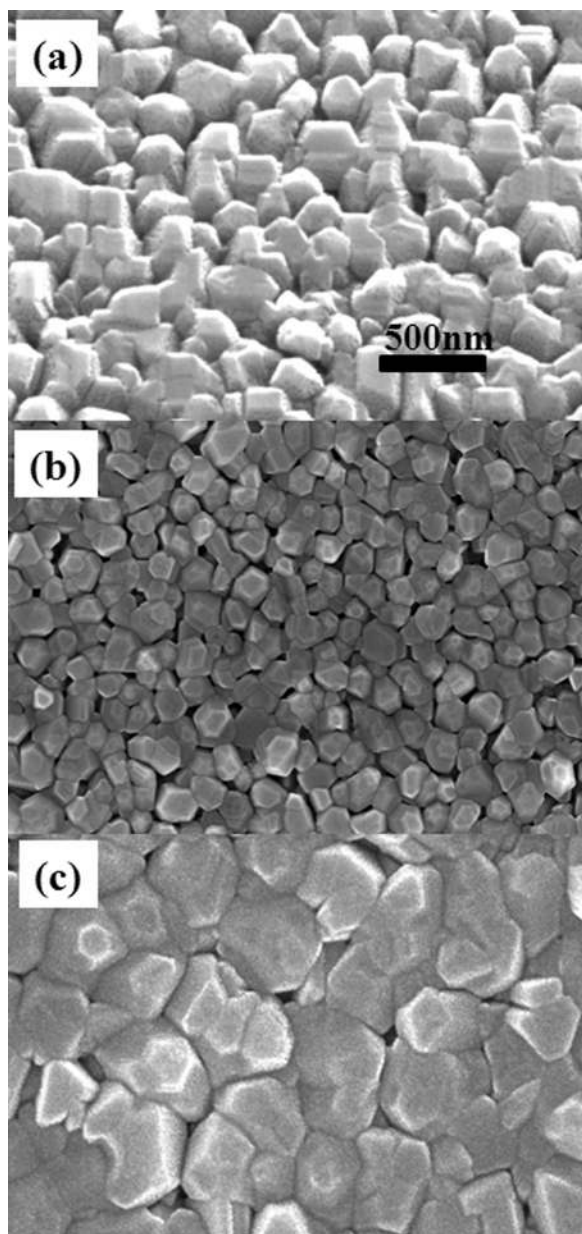


FIG. 2. SEM images of the GaN films grown with (a) absence of nitridation, (b) nitridation at 600 °C, and (c) nitridation at 800 °C.

PL spectroscopy was performed to investigate the optical transitions; hence the quality of the GaN films grown at different substrate nitridation conditions. Figure 4 shows the RT PL spectra for all the three samples. These spectra show a strong emission peak at 3.44 eV corresponding of the free excitonic (FX) transition. The narrow linewidth, such as 90 meV was observed for the sample grown with high temperature substrate nitridation. This linewidth is comparable to the previous report of GaN grown on Si (100) with the AlN buffer layer.¹⁰ For the other two samples the FWHM was found to be higher due to the reduced crystallinity compared to the sample grown with high temperature nitridation. Along with the FX peak, the donor acceptor pair (DAP) transition was also observed at the energy of 3.26 eV, which is attributed to a transition from shallow donor to shallow acceptor. This transition indicates that the samples are

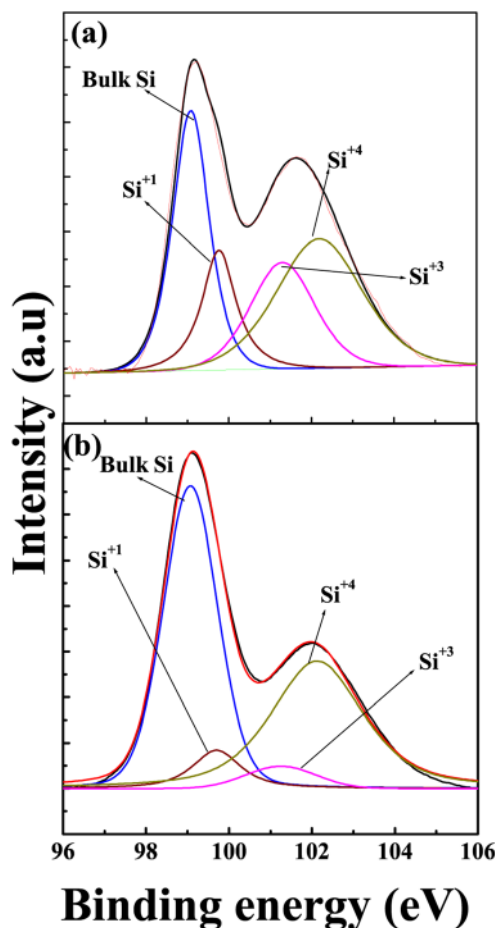


FIG. 3. (Color online) Si 2p core-level spectra of silicon nitride layers formed on the Si (100) surface at the nitridation temperatures of (a) 600 °C and (b) 800 °C.

unintentionally doped. A significant redshift in the DAP peak was observed in the sample with mixed phase. This shift might be due to the contribution of the lower bandgap of the cubic GaN (3.2 eV).¹¹ No yellow luminescence (YL) was found in any of the samples.

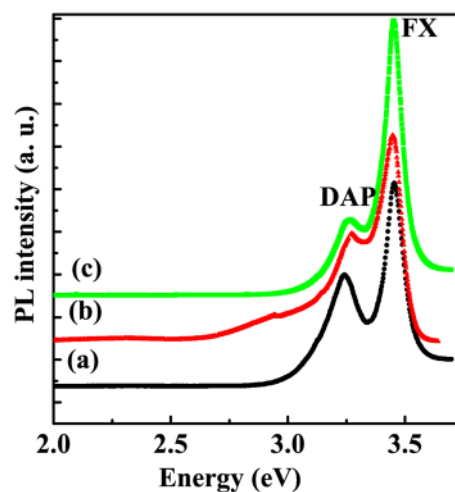


FIG. 4. (Color online) Room temperature photoluminescence spectra of the GaN films grown with (a) absence of nitridation, (b) nitridation at 600 °C, and (c) nitridation at 800 °C.

The I - V characteristics of n-GaN/p-Si heterojunctions exhibit an interesting inverted rectification behavior irrespective of nitridation conditions. This type of behavior was also found in p-ZnO/n-Si heterojunctions elsewhere.¹² The possible band alignment diagram of n-GaN/p-Si is shown in Fig. 5, certainly abnegates the possibility of interband tunneling. As we know, the bandgaps and electron affinities of Si and GaN are 1.12, 3.4, 4.05, and 3.1 eV,¹³ respectively, hence the conduction band offset, i.e., $\chi_{\text{GaN}} - \chi_{\text{Si}} = \Delta E_c$ (0.95 eV) is much smaller than the valence band offset, i.e., $\Delta E_v = \Delta E_g - \Delta E_c$ (1.33 eV). A quantum well for electrons is formed on the p-Si side as shown in the band alignment diagram. The Si is inverted in the interface when connecting to n-GaN. Hence, during the forward operation (positive bias on n-GaN) of the heterojunction diode electrons would overcome the Schottky barrier (i.e., effective band offset in the conduction band edge or the Fermi level in the inverted Si quantum well to the conduction band edge of GaN in the interface). In other words, the negative voltage polarity on p-Si results in the rectifying characteristics along with the transport of electrons from Si to GaN. These diodes behave like “n-type” Schottky diode due to dominated electron transport rather than bipolar transport in a regular p-n junction diode. Here the smaller bandgap material Si is comparable to the metal and the conduction band offset is equivalent to a Schottky barrier in an n-type diode. The reverse operation (positive bias on p-Si) results in a saturated current in the forward bias such as the reverse bias characteristic of a normal diode.

RT current voltage (I - V) characteristics of the GaN/p-Si (100) heterojunctions were measured and the behavior is shown in Fig. 6. The ohmic nature of the aluminum contact with Si as well as GaN was confirmed. All three diodes exhibit the turn on voltage of about 0.4 V, but the allowing current at turn on voltage is strongly dependent on the nitridation conditions. Samples grown in the absence of substrate nitridation and low temperature nitridation allows the current in the order of 10^{-4} A and 10^{-5} A, respectively. The non-stoichiometric Si_xN_y layer present in the sample with low temperature substrate nitridation acts as a thin insulator layer which reduces the current flow. Both the diodes show similar rectifying behavior with the on/off ratio of ~ 11 at 3 V. But

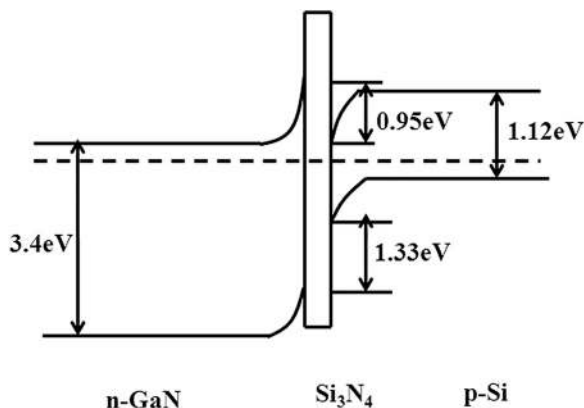


FIG. 5. Schematic energy band alignment diagram of the n-GaN/ Si_3N_4 /p-Si heterojunction under thermal equilibrium.

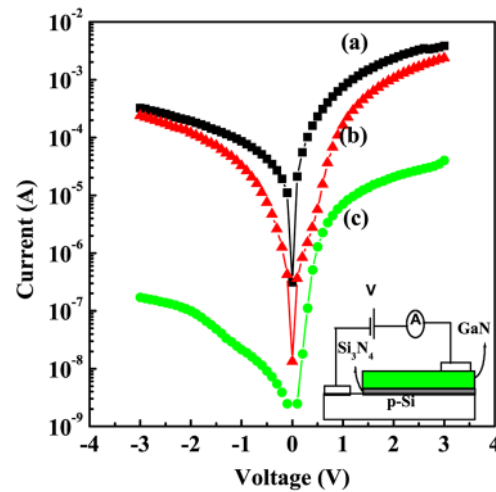


FIG. 6. (Color online) Room temperature I - V characteristics of the GaN/p-Si heterojunctions grown with (a) absence of nitridation, (b) nitridation at 600°C , and (c) nitridation at 800°C .

the diode with high temperature substrate nitridation exhibits a current of 10^{-6} A at the turn on voltage. Though it shows a noticeable reduction in the forward current, it exhibits the best rectifying behavior with on/off ratio ~ 230 at 3 V. The leakage current in this diode was found to be in the order of 10^{-7} A. A drastic reduction in the leakage current is attributed to the low defect concentration or trap centers in the film or interfacial layer due the introduction of stoichiometric Si_3N_4 buffer layer.

The I - V curves of all the three diodes were fitted at low voltage regions (< 0.5 V) by using the standard diode equation,

$$I = I_s \left[\exp\left(\frac{qV}{\eta kT}\right) - 1 \right]. \quad (1)$$

The diode grown with the absence of substrate nitridation showed the highest ideality factor, $\eta \sim 6$ and the diode fabricated with low temperature substrate nitridation resulted in an ideality factor of ~ 4 . The ideality factors greater than 2 indicate a nonideal nature of the diodes. The high ideality factor often attributed to the presence of defect states which causes the deep level assisted tunneling¹⁴ or lateral in homogeneities of the barrier height at the interfaces.¹⁵ The diode fabricated with high temperature substrate nitridation showed an ideality factor ~ 1.5 . This behavior clearly shows transport is governed by the recombination at space charge region mechanism at low voltages.

The saturation current (I_s) should have the form,

$$I_s = AA^* T^2 \exp\left(-\frac{\phi_b}{kT}\right) \quad (2)$$

according to the thermionic emission model, where A is the contact area of the junction, A^* is the Richardson constant ($112 \text{ A cm}^{-2} \text{ K}^{-2}$ for n-Si, due to inverted rectification¹⁶), and ϕ_b is the effective barrier height. At RT ϕ_b is obtained to be 0.63 eV, 0.71 eV, 0.82 eV for the diodes grown with the absence of nitridation, low temperature nitridation, and high

temperature nitridation, respectively. Obtained barrier height values confirm the tunneling of carriers in the samples grown without nitridation as well as low temperature nitridation. Further, the barrier height observed in the case of heterojunctions grown with high temperature nitridation, i.e., 0.82 eV is in close agreement with the conduction band offset of GaN/Si heterojunction i.e., 0.95 eV, which abnegates the thermally generated carrier tunneling.

For the further investigation of transport mechanisms at lower as well as higher voltages, the log-log plots of the room temperature forward I - V data have been studied. Figure 7 shows the log-log plot of the three diodes of different nitridation conditions. Three distinct regions were observed depending on the applied voltage, which were assigned as region I, II, III. At low forward voltage (region I), the current transport follows a linear ohmic behavior ($I \propto V$) which is attributed to the thermally generated carrier tunneling.¹⁷ The region I for the heterojunction grown in absence of nitridation is much wider than that of the samples grown with substrate nitridation, and regions II and III were not observed. This behavior may also be caused by the presence of a large trap concentration. In the sample grown with low temperature nitridation, the observed region I is very short (< 0.3 V) and region II was observed in the range of 0.3–0.8 V, in which the current increases exponentially and follows a relation of $I \sim \exp(\alpha V)$, and is attributed to the recombination tunneling mechanism which is frequently observed in wide bandgap heterojunctions.¹⁷ In the sample grown with high temperature nitridation the region I was not observed which indicates that the drastic reduction in the trap concentration due to the increase in the quality of the silicon nitride layer and hence of the GaN layers and region II was observed in the voltage range of $V < 0.4$ V. The constant α can be given as

$$\alpha = (8\pi/2h)(m_h * \epsilon_s)^{1/2} N_D / [N_A^{1/2} (N_A + N_D)], \quad (3)$$

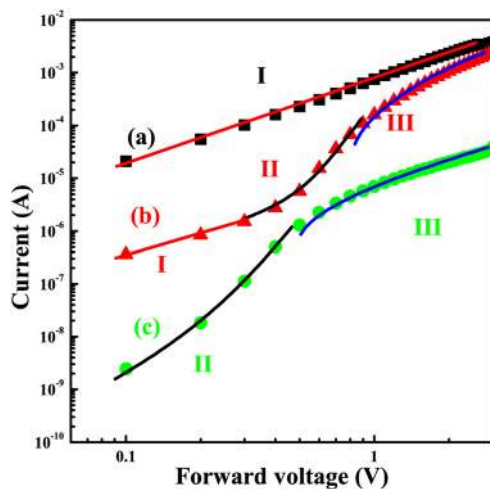


FIG. 7. (Color online) Log-log plots of the current-voltage characteristic under forward bias for diodes grown with (a) the absence of nitridation, (b) low temperature nitridation, and (c) high temperature nitridation.

where h is Planck's constant, m_h^* is the effective mass of holes, ϵ_s is the dielectric constant of GaN, N_D is the donor concentration of GaN films, N_A is the acceptor concentration of the p-Si substrate. By fitting region II of the curves, α is evaluated to be 14 V^{-1} and 15 V^{-1} for the devices fabricated with low temperature substrate nitridation and high temperature substrate nitridation, respectively. A larger value of α indicates higher carrier injection. This region signifies the injected carriers will exceed the thermally generated carriers and fill the unoccupied traps.¹⁷

In the substrate nitrided samples the region III was well pronounced in which the current follows the dependence of $I \sim V^2$. This square law dependence is generally observed in the wide bandgap semiconductors and it is reported to be attributed to the space-charge-limited current (SCLC) conduction. The similar conduction mechanisms have been observed by Shen *et al.*¹⁸ and Liu *et al.*¹⁷ for their GaN Schottky diodes and n-ZnO nanorods/p-Si heterojunction diodes, respectively. The SCLC phenomenon is caused by the different offsets of the conduction band and valence band at the junction interface of n-GaN and p-Si as shown in the n-GaN/p-Si band alignment diagram in Fig. 5. (Though the formation of Si_3N_4 layer is intentional, thickness must be very low, confirmed by the XPS. A systematic TEM studies done by Yang *et al.*⁶ also reports the low thickness (< 5 nm) of the Si_3N_4 layer. The Si_3N_4 layer is located at the space charge region of the n-GaN/p-Si diode; it would certainly allow the carriers to tunnel through.) The energetic barrier for electrons is less than the barrier for holes. So the injection current is dominated by the injected electrons under the forward voltage and the single carrier current forms as shown in Fig. 5. Further, when the injected carriers completely fill all the traps, the injected current follows the square law SCLC behavior. The sample with the absence of substrate nitridation does not show the SCLC behavior. The sample with low temperature nitridation follows the SCLC behavior after the forward bias gets to 0.9 V and for the sample with high temperature nitridation is 0.5, which means that more traps exist in the sample with the absence of nitridation and a larger trap filled limit voltage (V_{TFL}) is required to completely fill these traps.¹⁹ Whereas, the samples with nitridation, shows a rapid transition from exponential to SCLC region and V_{TFL} is much smaller than the sample with the absence of nitridation, which can be attributed to the presence of fewer traps and larger injection of carriers.

CONCLUSIONS

The effect of substrate nitridation and nitridation temperature on the growth and properties of GaN epilayers on the Si (100) substrate by MBE has been studied. The GaN films grown directly on Si (100) substrates contain mixed phases, i.e., wurtzite along with the zinc blende, which was confirmed by XRD and PL results. Nitridation of Si surface favors the growth of phase pure wurtzite GaN on it. Core-level photoelectron spectroscopy of silicon nitride layers reveal the sources for the superior quality of GaN epilayers grown with the high temperature substrate nitridation process. Typical inverted rectification behavior of the

n-GaN/p-Si heterojunction had been discussed. A systematic variation in the barrier heights as well as in the ideality factors obtained for GaN/p-Si heterojunctions confirms the modulations in transport mechanisms with different nitridation conditions. The heterojunctions grown in the absence of substrate nitridation exhibits thermally generated carrier tunneling as the dominating transport mechanism and the defects present in the lattice and interfaces act as nonradiative centers to reduce the UV emission and also work as trap centers to capture the injected electrons and degrade the injection current. In the case of low temperature substrate nitridation, though the intensity of UV emission has improved and ideality factors were reduced (~ 4), the existence of the trap centers was confirmed. The recombination tunneling is the major transport mechanism at higher voltages. The high temperature substrate nitridation certainly reduced the structural imperfections as well as shallow or deep traps in the energy band; as a consequence the crystalline quality of the GaN films was increased indicated by XRD and band to band emission in the PL spectra. The sharp and narrow linewidth of the PL shows the reasonably low intrinsic carrier density and high crystalline quality. This improved the electrical transport performance of the heterojunction. At the low voltages recombination tunneling at the space charge region is the transport mechanism and at higher voltages space charge limited current conduction is the dominating transport mechanism.

- ¹B. Yang, O. Brandt, A. Trampert, B. Jenichen, and K. H. Ploog, *Appl. Surf. Sci.* **123**, 1 (1998).
- ²S. Joblot, F. Semond, Y. Cordier, P. Lorenzini, and J. Massies, *Appl. Phys. Lett.* **87**, 133505 (2005).
- ³Y. Nakada, I. Aksenov, and H. Okumura, *Appl. Phys. Lett.* **73**, 827 (1998).
- ⁴J. X. Zhang, Y. Qu, Y. Z. Chen, A. Uddin, P. Chen, and S. J. Chua, *Thin Solid Films* **515**, 4397 (2007).
- ⁵M. Kumar, T. N. Bhat, M. K. Rajpalke, B. Roul, N. Sinha, A. T. Kalghatgi, and S. B. Krupanidhi, *Solid State Commun.* **151**, 356 (2011).
- ⁶B. Yang, A. Trampert, O. Brandt, B. Jenichen, and K. H. Ploog, *J. Appl. Phys.* **83**, 3800 (1998).
- ⁷G. L. Zhao and M. Bachlechner, *Phys. Rev. B* **58**, 1887 (1998).
- ⁸J. Kim and H. Yeom, *Phys. Rev. B* **67**, 035304 (2003).
- ⁹H. M. Lee, C. T. Kuo, H. W. Shiu, C. H. Chen, and S. Gwo, *Appl. Phys. Lett.* **95**, 222104 (2009).
- ¹⁰J. Wan, R. Venugopal, M. R. Melloch, H. M. Liaw, and W. J. Rummel, *Appl. Phys. Lett.* **79**, 1459 (2001).
- ¹¹Hadis Morkoz, *Handbook of Nitride Semiconductors and Devices* (Wiley-VCH, New York, 2008), Vol. 2.
- ¹²L. J. Mandalapu, F. X. Xiu, Z. Yang, and J. L. Liu, *J. Appl. Phys.* **102**, 023716 (2007).
- ¹³T. E. Cook, Jr., C. C. Fulton, W. J. Mecoouch, R. F. Davis, G. Lucovsky, and R. J. Nemanich, *J. Appl. Phys.* **94**, 3949 (2003).
- ¹⁴H. C. Casey, Jr., J. Muth, S. Krishnakutty, and J. M. Zavada, *Appl. Phys. Lett.* **68**, 2867 (1996).
- ¹⁵J. H. Werner and H. H. Güttler, *J. Appl. Phys.* **69**, 1522 (1991).
- ¹⁶A. Domaingo and F. Schürer, *Semicond. Sci. Technol.* **21**, 429 (2006).
- ¹⁷S. Y. Liu, T. Chen, Y. L. Jiang, G. P. Ru, and X. P. Qu, *J. Appl. Phys.* **105**, 114504 (2009).
- ¹⁸X. M. Shen, D. G. Zhao, Z. S. Liu, Z. F. Hu, H. Yang, and J. W. Liang, *Solid-State Electron.* **49**, 847 (2005).
- ¹⁹X. D. Chen, C. C. Ling, S. Fung, C. D. Beling, Y. F. Mei, K. Ricky, Y. Fu, G. G. Siu, and P. K. Chu, *Appl. Phys. Lett.* **88**, 132104 (2006).